Chemical Science

ROYAL SOCIETY OF CHEMISTRY

EDGE ARTICLE

View Article Online
View Journal | View Issue

Check for updates

Cite this: *Chem. Sci.*, 2021, **12**, 2549

All publication charges for this article have been paid for by the Royal Society of Chemistry

Received 11th November 2020
Accepted 28th December 2020

DOI: 10.1039/d0sc06219g

rsc.li/chemical-science

Development of isotope-enriched phosphatidylinositol-4- and 5-phosphate cellular mass spectrometry probes†

Amélie M. Joffrin,[a] Alex M. Saunders,[a] David Barneda,[bc] Vikki Flemington,[c] Amber L. Thompson,[a] Hitesh J. Sanganee[d] and Stuart J. Conway *[a]

Synthetic phosphatidylinositol phosphate (PtdInsP_n) derivatives play a pivotal role in broadening our understanding of PtdInsP_n metabolism. However, the development of such tools is reliant on efficient enantioselective and regioselective synthetic strategies. Here we report the development of a divergent synthetic route applicable to the synthesis of deuterated PtdIns4*P* and PtdIns5*P* derivatives. The synthetic strategy developed involves a key enzymatic desymmetrisation step using Lipozyme TL-IM®. In addition, we optimised the large-scale synthesis of deuterated *myo*-inositol, allowing for the preparation of a series of saturated and unsaturated deuterated PtdIns4*P* and PtdIns5*P* derivatives. Experiments in MCF7 cells demonstrated that these deuterated probes enable quantification of the corresponding endogenous phospholipids in a cellular setting. Overall, these deuterated probes will be powerful tools to help improve our understanding of the role played by PtdInsP_n in physiology and disease.

Introduction

Phosphatidylinositol phosphates (PtdInsP_ns) are a family of minor membrane phospholipids that regulate a diverse range of important intracellular processes, including membrane trafficking, plasma membrane receptor signalling, cell proliferation, metabolism, and transcription.[1,2] Structurally, PtdIns comprise a *myo*-inositol headgroup that is linked at the 1-position to the *sn*-3 position of a diacylglycerol backbone *via* a phosphodiester bridge.[3] Reversible phosphorylation at the 3-, 4- and/or 5-position of the PtdIns headgroup is tightly regulated by a series of kinases and phosphatases.[2,4] The resulting set of seven PtdInsP_ns participate in intracellular signalling pathways,[5,6] at membrane–cytosol interfaces, by interacting with integral membrane proteins or by recruiting effector proteins.[7,8] Importantly, each PtdInsP_n is characterised by a distinct subcellular distribution and biological function,[2,9] and therefore contribute to defining organelle identity.[10]

Dysregulation of phosphoinositide metabolism and signalling is associated with a number of conditions including inflammation, cancer, and neurological disorders.[11] Notably, phosphatidyl inositol 4-kinase (PtdIns4K) isozymes have been recognised as potential therapeutic targets in a variety of disease settings, including RNA viruses and Alzheimer's disease.[12,13] However, pharmacological manipulation of the subcellular levels of PtdIns4*P* is particularly challenging[14] due to the lack of information on the isoform-specific roles and localisation of PtdIns4K.[17,18] Furthermore, the metabolism and function of less abundant PtdInsP_ns are still poorly understood. For instance, PtdIns5*P* has recently been proposed to mediate nuclear signalling events and chromatin remodelling.[15] Despite its importance in epigenetics, the localisation and dynamics of PtdIns5*P* remains to be established, mostly due to the lack of methods to visualise and quantify subcellular levels of this low abundance phosphoinositide.

A number of tools and technologies have been developed to address important questions in PtdInsP_n biology. PtdInsP_n derivatives that encompass fluorescent reporter groups,[16,17] provide information on PtdInsP_n activity and localisation. Relevant PtdInsP_n binding partners can also be identified using immobilised analogues and photoaffinity-based probes.[16–19] These chemical probes, however, contain a reporter group appended to the lipid backbone. Such a bulky modification has profound effects on the properties of the lipids. In addition, recent evidence suggests that the nature of the PtdInsP_ns lipids is of particular importance.[20,21] For instance, enrichment of PtdInsP_ns with 1-stearoyl-2-arachidonyl lipid chains in mammals affects which proteins they interact with in cells. In an attempt to elucidate the functional significance of different fatty-acyl species, integrated high-performance liquid

[a]*Department of Chemistry, Chemistry Research Laboratory, University of Oxford, Mansfield Road, Oxford OX1 3TA, UK. E-mail: stuart.conway@chem.ox.ac.uk*
[b]*Inositide Laboratory, Babraham Institute, Babraham Research Campus, Cambridge, CB22 3AT, UK*
[c]*Bioscience, Oncology R&D, AstraZeneca, Cambridge, CB4 0WG, UK*
[d]*Discovery Sciences, BioPharmaceuticals R&D, AstraZeneca, Cambridge, UK*

† Electronic supplementary information (ESI) available: Experimental procedures, NMR and X-ray crystallographic data. CCDC 2049548 and 2049549. For ESI and crystallographic data in CIF or other electronic format see DOI: 10.1039/d0sc06219g

chromatography-mass spectrometry (HPLC-MS)-based methodologies have been developed. While these techniques enable the absolute and relative measurements of subcellular PtdIns*P*, PtdInsP_2, and PtdInsP_3 levels,[22,23] the PtdInsP_n positional isomers, cannot be distinguished.

Stable-isotope-enriched inositol derivatives, including PtdInsP_ns, would represent invaluable chemical probes for addressing the shortcomings of existing methodologies. Indeed, stable isotope-labelled biomolecules have become powerful tools in a range of analytical assays, as exogenously supplied metabolic tracers, or as mass-spectrometry internal standards.[24] Furthermore, there has recently been a rapid advance in the development of methodologies harnessing stable isotope labelled probes.[25] Notably, innovative imaging technologies using D- or ^{13}C-labeled metabolites enable metabolism mapping at the single cell level.[26,27] Despite this, the synthesis of PtdInsP_ns is particularly challenging. Due to the *meso* nature of *myo*-inositol **1**, both stereo- and regiocontrol are required for the synthesis of most inositol derivatives. In addition, previously developed synthetic routes typically involve diastereoisomeric resolutions, are often only applicable to the synthesis of saturated PtdInsP_n derivatives, and can suffer from poor overall yields. These routes are therefore not applicable to the synthesis of expensive isotope-enriched materials.[28–32] Given the high cost of isotopically labelled materials, synthetic routes must be as concise as possible, scalable, and reproducible.

Here we report the streamlined synthesis of PtdIns4*P* and PtdIns5*P* using a key enzymatic desymmetrisation step. This divergent synthetic route is robust and high yielding, and thus applicable to the synthesis of a wide range of stable isotope-enriched PtdIns4*P* or PtdIns5*P* analogues (Fig. 1). The new methods described in this work will enable the expedient synthesis of a subset of powerful isotopically-enriched chemical tools to address key questions in PtdIns4*P* and PtdIns5*P* biology.

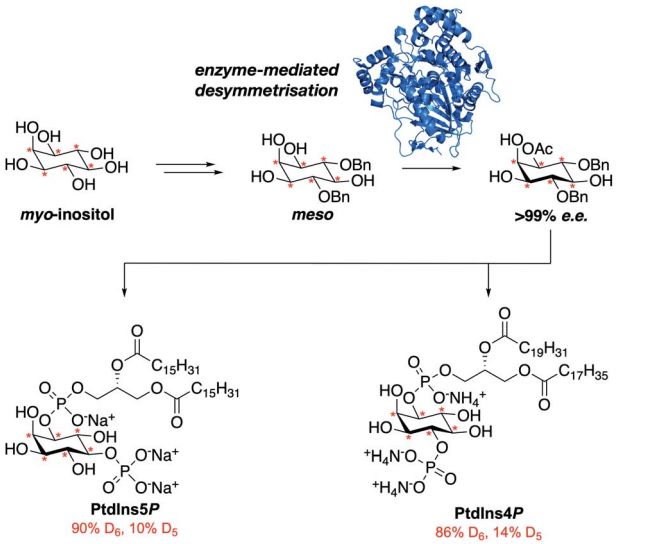

Fig. 1 The streamlined synthesis of PtdIns4*P* and PtdIns5*P* using a key enzymatic desymmetrisation step. ✱ = deuterium.

Results and discussion

Retrosynthetic analysis

Our main aim was to develop a high yielding and modular synthetic route to give enantiomerically pure PtdIns4*P* and PtdIns5*P*. We envisaged that the fully protected PtdIns4*P* and PtdIns5*P* precursors **2** and **3** would be obtained by assembly of two main fragments: the enantiomerically-pure and orthogonally-protected *myo*-inositol cores **4** and **5**, and the phosphoramidite **6** derivatised with a range of saturated and unsaturated lipid chains (Scheme 1). The first consideration for the synthesis of *myo*-inositol cores **4** and **5**, was the optimisation of a high yielding desymmetrisation step.

In addition to the elegant work by Miller and co-workers,[33–35] a few studies have reported efficient desymmetrisations of 4,6-di-*O*-benzyl ether protected *myo*-inositol derivatives, to provide 1-*O*- or 3-*O*-acyl derivatives such as **9**.[36–39] Indeed, differentiation between the enantiotopic 1- and 3-*O*-positions of the *myo*-inositol ring is known to be promoted by the stereochemical environment of these positions, which comprise both neighbouring axial and equatorial substituents. Furthermore, differentiation at the 1-*O*-position is advantageous for the synthesis of PtdInsP_ns, as this eliminates the need for a low yielding, regioselective transformation at this position. We also envisaged that protection of the 2,3-diol would provide PtdIns5*P*

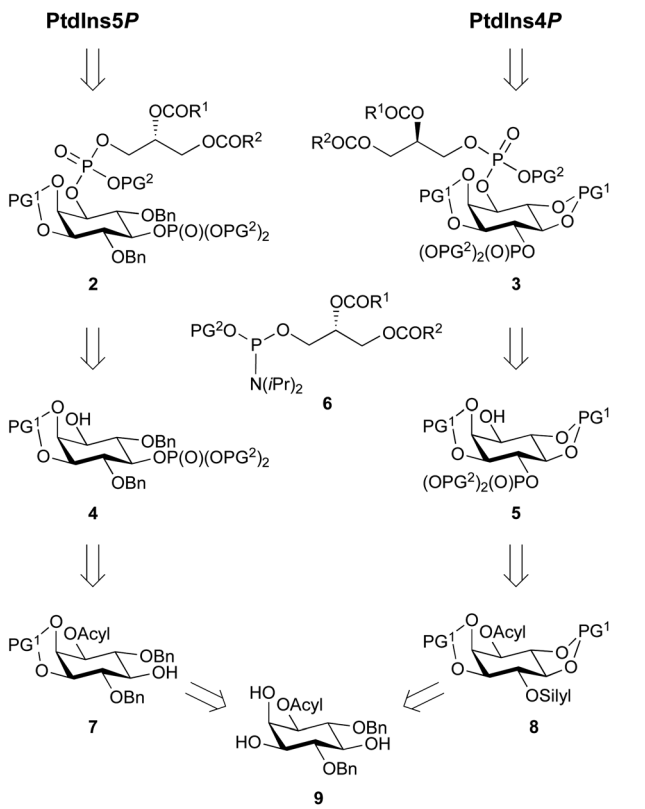

Scheme 1 Retrosynthetic analysis for PtdIns4*P* and PtdIn5*P*. PG^1 = acid labile protecting group; PG^2 = alkyl phosphate ester protecting group; R^1 and R^1 = saturated or unsaturated lipid chains. Bn = benzyl.

precursor **7**, without the need for further protecting group manipulations.

Another important consideration is the nature of the hydroxyl and phosphate protecting groups employed, and their compatibility with global deprotection of the sensitive final molecule. We selected benzyl- or 1,2-xylene-derived esters (PG^2) to protect the phosphate groups and acid-labile groups (PG^1) to protect positions around the desymmetrised *myo*-inositol ring. Indeed, previous work had shown that these could be simultaneously removed in a global deprotection step under mild conditions.[30,33,40] In addition, acyl groups can be efficiently deprotected in the presence of alkyl phosphate esters.[41]

To synthesise a suitable PtdIns4*P* intermediate, we hypothesised that selective protection of the 4-*O*-position with an orthogonal silyl protecting group (silyl), would be achievable after cleavage of the 4,6-*O*-ether groups. Subsequent protection of the 5- and 6-*O*-positions with acid-labile groups (PG^1) would provide **8**, with the desired differentiated 1- and 4-*O*-positions of the inositol ring. Finally, we postulated that selective silyl deprotection and phosphorylation would give PtdIns4*P* precursor **5** (Scheme 1).

Synthesis of enantiomerically pure building block (−)-9

Our investigation started with the optimisation of an appropriate desymmetrisation strategy to give orthogonally protected PtdIns4*P* and PtdIns5*P* building blocks **7** and **8**. First, we prepared *meso*-4,6-di-*O*-benzyl-*myo*-inositol **15** from *myo*-inositol **1**, as described in the literature.[42,43] Briefly, reaction of *myo*-inositol **1** with triethylorthoformate and substoichiometric PTSA·H_2O in DMF gave the inositol orthoformate **11** in a 65% yield. Regioselective dialkylation of the axial positions on **11** provided the 4,6-di-*O*-benzylated derivative **13** as the major product.[44] Subsequent methanolysis of this orthoformate, using PTSA·H_2O in methanol, furnished **15** (Scheme 2). Next, differentiation between the enantiotopic 1- and 3-*O*-positions of this *meso* intermediate was achieved *via* an enantioselective desymmetrisation catalysed by the lipase from *Thermomyces lanuginosus*, Lipozyme TL-IM®.[45] Following the procedure reported by Simas *et al.*,[37] **15** was stirred with Lipozyme TL-IM® in hexane and vinyl acetate at 45 °C for 15 hours, generating the desired acetylated product (−)-**9** in 98% yield (Scheme 2). The racemate (±)-**9** was prepared under standard conditions, and analysis using chiral HPLC revealed that the e.e. of (−)-**9** was greater than 99% (Fig. S1†). We found that this enzymatic transformation is also applicable to 4,6-di-*O*-(4-methoxybenzyl) derivatives (Fig. S3 and Scheme S2†). Importantly, these desymmetrisations can be carried out on gram scale, without concurrent reduction of the yields or e.e. values (Fig. S1 and S3†).

Next, the 2- and 3-*O*-position of (−)-**9** were simultaneously protected with the acid labile cyclopentylidene group, using **18**, to provide (−)-**19** in 92% yield (Scheme 2). Assignment of the absolute configuration of the protected derivative (−)-**19** was undertaken by ^{1}H NMR analysis of the corresponding (*R*)- and (*S*)-methoxyphenylacetic acid (MPA) esters (ESI Results and discussion 4.1†).[46] Based on this study, the absolute configuration of (−)-**9** was assigned as (−)-1D-1-*O*-acetyl-4,6-di-*O*-benzyl-*myo*-inositol, which is in agreement with previous work.[47] Thus, enantioselective acetylation at the 1-*O*-position of 4,6-di-*O*-protected *myo*-inositols can be achieved enzymatically, providing the versatile PtdInsP_n precursor (−)-**9**.

Synthesis of deuterated *myo*-inositol 10

Having completed the enantioselective desymmetrisation of **15** with Lipozyme TL-IM®[37] and confirmed the absolute configuration of (−)-**9**, we considered the applicability of this methodology to stable isotope-enriched *myo*-inositol derivatives. While a low-cost and large-scale synthesis of [$^{13}C_6$]-*myo*-inositol had previously been reported by the Fiedler group,[25] the cost of D_6-*myo*-inositol **10** remains prohibitively high. Indeed, previously reported synthetic routes required laborious separation of epimers.[48] To expand the scope of isotope-enriched *myo*-inositol derivatives applicable to our synthesis, we developed a robust and efficient multi-gram synthesis of D_6-*myo*-inositol.

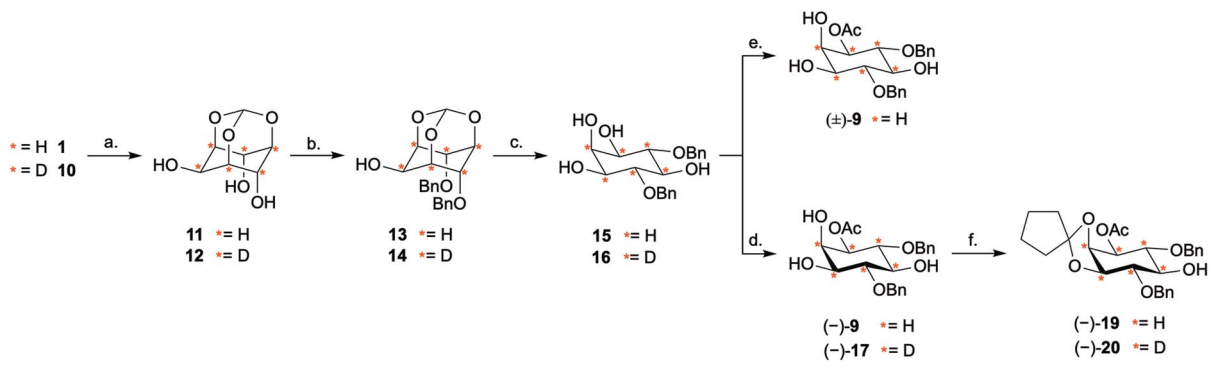

Scheme 2 Synthesis of enantiomerically pure (−)-**19** and D_6 (−)-**20** *via* an enzymatic desymmetrisation step using Lipozyme TL-IM®. *Reagents and conditions*: (a) $CH(OEt)_3$, PTSA·H_2O, DMF, 105 °C, 3 d, 65% **11**; 7 d, 31%, 89% D_6, 11% D_5, D_6 **12**. (b) (i) LiH, DMF, RT, 30 min, (ii) BnBr, RT, 48 h, 71% **13**; 77%, 91% D_6, 9% D_5, D_6 **14**. (c) PTSA·H_2O, MeOH, RT, 24 h, 92% **15**; 86%, 92% D_6, 8% D_5, D_6 **16**. (d) Lipozyme TL-IM®, vinyl acetate/hexane (1 : 1), 45 °C, 15 h, 98%, >99% e.e. (−)-**9**; 84%, >99% e.e., 89% D_6, 11% D_5, D_6 (−)-**17**. (e) Ac_2O, Et_3N, 4-DMAP, CH_2Cl_2, −20 °C to −10 °C, 30 h, 7% (±)-**9**. (f) 1,1-Dimethoxycyclopentane **18**, PTSA·H_2O, CH_2Cl_2, RT, 18 h, 92% (−)-**19**; 87%, 91% D_6, 9% D_5, D_6 (−)-**20**. Ac = acetyl; Bn = benzyl; 4-DMAP = 4-dimethylaminopyridine; DMF = dimethylformamide; PTSA = 4-toluene sulfonic acid; * = deuterium.

We began this synthesis from quinol **21**, as its deuterated analogues can be readily synthesised, and converted into *myo*-inositol derivatives. Following a procedure reported by Zimmermann *et al.*, quinol **21** was treated with D_2SO_4 in D_2O, and the deuterated quinol **22** generated was isolated by extraction with Et_2O (Scheme 3).[49] This procedure was repeated three times to give an overall incorporation of 93% D_4 and 7% D_3 (Scheme 3). Deuterated quinol **22** was then oxidised using aqueous H_2O_2 in isopropanol with catalytic iodine at 45 °C,[50] providing pure D_4 *p*-benzoquinone **23** in 85% yield over two steps, with no loss of deuterium incorporation (Scheme 3, 93% D_4, 7% D_3). D_4-*p*-Benzoquinone **23** was then brominated using Br_2 and reduced with $NaBD_4$ to give (±)-**25**. Subsequent reaction under conditions reported by Trost *et al.* produced (±)-**26** with a 90% D_6- and 10% D_5-enrichment.[51] The structure of (±)-**26** was confirmed using single crystal X-ray diffraction studies (Fig. 2A, ESI†). Intermediate (±)-**26** was subsequently subjected to a *syn*-dihydroxylation to produce the tetracetylinositol derivative (±)-**27** (Scheme 3). Analysis of the crude reaction mixture obtained from this transformation revealed that acetyl migration had occurred to give an inseparable mixture of (±)-**27** and (±)-**28**. Acetyl deprotection of this mixture and crystallisation provided D_6-*myo*-inositol **10**. Given the nature of the ^1H and ^{13}C NMR spectra obtained for these deuterated molecules, the protonated analogues were synthesised in a similar manner and used to aid structure confirmation (ESI†). This novel synthetic route therefore allows for the synthesis of D_6-*myo*-inositol with high isotopic enrichment (84–90% D_6, 10–16% D_5) on a gram scale and at low cost.

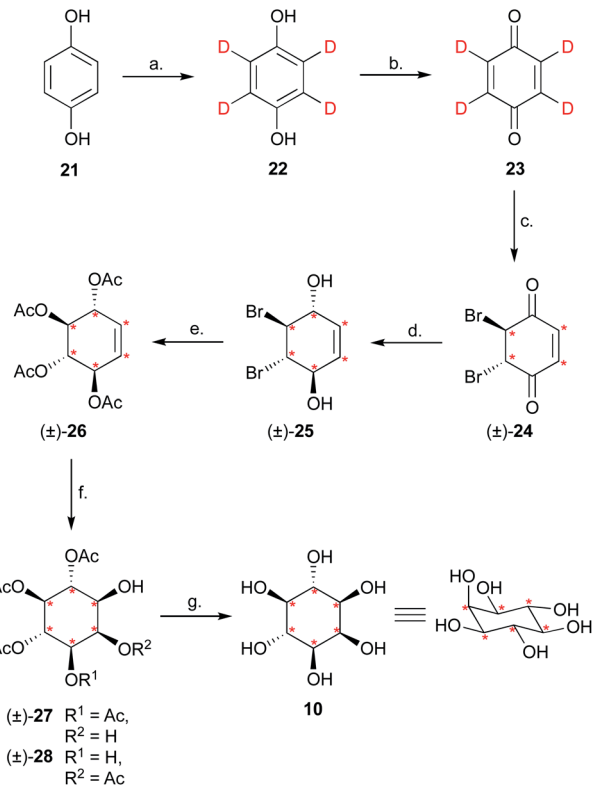

Scheme 3 Synthesis of D_6-*myo*-inositol **10**. *Reagents and conditions*: (a) D_2SO_4, D_2O, reflux, 3 × 24 h, 95%, D_4 93%, D_3 7%. (b) 35% w/w $H_2O_{2(aq)}$, I_2, ^iPrOH, 45 °C, 2 h, 89%, 93% D_4, 7% D_3. (c) Br_2, $CHCl_3$, 0 °C, 3 h. (d) $NaBD_4$, D_2O, Et_2O, 0 °C, 2 h. (e) (i) Ac_2O, K_2CO_3, 2 h, (ii) AcOH, reflux, 45 h, 29% over 3 steps, 90% D_6, 10% D_5. (f) $NaIO_3$, $RuCl_3 \cdot H_2O$, MeCN, H_2O, 0 °C, 4–8 min. (g) Et_3N, MeOH/H_2O, RT, 2 h, 55% over 2 steps, 84–90% D_6, 10–16% D_5. Ac = acetyl; ✱ = deuterium.

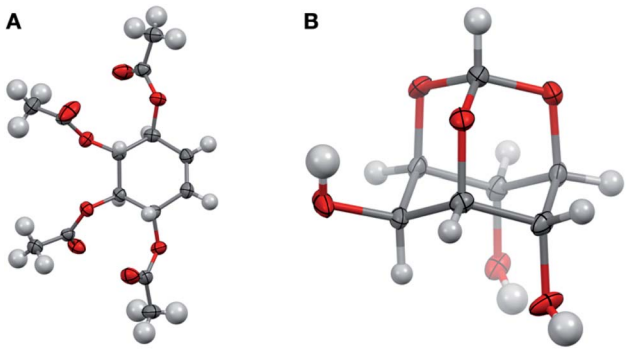

Fig. 2 Structures of D_6-(±)-**26** ((A) CCDC 2049549) and orthoformate D_6-**12** ((B) CCDC 2049548) from single crystal X-ray diffraction studies (ESI†) Key: carbon, grey; oxygen red; hydrogen or deuterium, white, displacement ellipsoids drawn at 50% probability.

Synthesis of deuterated intermediate (−)-20

Next, we explored whether D_6-*myo*-inositol **10** could be used as a starting material for the synthesis of D_6-*meso*-4,6-di-substituted *myo*-inositols **16**, and whether Lipozyme TL-IM® could tolerate the desymmetrisation of deuterated inositol derivatives. Similar to the synthesis of H_6-(−)-**9**, D_6-*myo*-inositol **10** was converted to the corresponding D_6-inositol orthoformate **12** (Scheme 2), and the structure of this compound was established using single crystal X-ray diffraction (Fig. 2B, ESI†). However, this reaction was slow and, after seven days stirring at 105 °C, significant amounts of starting material remained. Although low yields were obtained (31%), mass spectrometry studies showed that there had been no change in the deuterium incorporation (89% D_6, 11% D_5). Importantly, the remaining starting material was recovered (45%) and could be recycled. The inositol ring undergoes a conformational flip to enable formation of a stable orthoformate structure. The observed difference in reaction efficiencies between protonated and deuterated material could be due to the shorter C–D bonds in **10**, resulting in a higher energy barrier to this conformational change. It is also possible that the slower reaction rate, and lower yield of **12** (compared to **11**), results from secondary kinetic isotope effects.

Regioselective alkylation of the 4- and 6-*O*-axial positions, followed by acidic methanolysis, proceeded smoothly to give *meso*-**16**. Desymmetrisation of this derivative using Lipozyme TL-IM® was successful, yielding (−)-**17** in 86% yield, without loss of deuterium incorporation. Notably, as for the protonated analogues, the e.e. of the acetylated product (−)-**17** was found to be >99% using chiral HPLC (Fig. S1†).

The deuterated intermediate (−)-**20** was obtained by protection of the 2- and 3-*O*-position of (−)-**17** with

a cyclopentylidene group. Overall, enzymatic desymmetrisation of H_6- and D_6-*meso*-4,6-di-substituted *myo*-inositols was accomplished to provide enantiomerically pure PtdIns4*P* and PtdIns5*P* precursors (−)-**19** and (−)-**20** in high yields.

Synthesis of saturated and unsaturated phosphoramidite fragments (+)-35, (+)-36, (+)-44 and (+)-45

We have developed a general approach for the synthesis of enantiomerically pure saturated and unsaturated phosphoramidite fragments, including (+)-**35**, (+)-**36**, (+)-**44** and (+)-**45**. This synthesis is shown in Scheme 4, and a full discussion is provided in the ESI (Results and discussion 4.2–4.3†).

Synthesis of dipalmitoyl PtdIns4*P*, D_6-dipalmitoyl PtdIns4*P*, D_{41}-distearoyl PtdIns4*P*, 1-stearoyl-2-arachidonoyl PtdIns4*P*, dipalmitoyl PtdIns5*P* and D_6-dipalmitoyl PtdIns5*P*

The synthesis of PtdIns4*P* derivatives commenced with the cleavage of the 4- and 6-*O*-benzyl ethers of (−)-**19**, *via* hydrogenolysis catalysed by 10% Pd/C under an atmosphere of $H_{2(g)}$ (Scheme 5). Conditions for regioselective protection of the 4-*O*-position of inositol ring (−)-**46** were then optimised (ESI Results and discussion 4.4†). While standard silylation conditions using *tert*-butyldimethylsilyl chloride (TBDMSCl) and imidazole were unsuccessful, the more reactive silylating agent TBDMSOTf led to the formation of the expected 4-*O*-silylated product (Table S3†). Regioselectivity of the reaction was further improved by using the bulkier TIPS group (Scheme S5†). The 4-*O*-TIPS ether (−)-**48** was thus obtained in 71% yield using TIPSOTf in the presence of 2,6-lutidine at −78 °C, and regioselectivity was confirmed by ^1H–^{29}Si Heteronuclear Multiple Bond Correlation (HMBC) NMR analysis (Fig. S4†).

Next, we postulated that a second cyclopentylidene moiety could be employed to mask the *trans*-5,6-diol on (−)-**48**. As expected for a *trans*-diequatorial diol, the rate of protection at these positions was slower than protection of the *cis* 2,3-diol. Despite this, the 2,3:5,6-di-*O*-cyclopentylidene acetal (−)-**50** was obtained in 85% yield by heating to 30 °C for 18 hours. This fully protected inositol derivative (−)-**50** was found to be unstable under desilylation conditions using $Et_3N{\cdot}3HF$. Furthermore, silyl deprotection using pyridine·HF facilitated partial intermolecular *trans*-esterification of the 1-*O*-acetyl ester (Table S4†). As an alternative, we found that the soluble, mild, and anhydrous source of nucleophilic fluoride, tris(dimethylamino) sulfonium difluorotrimethylsilicate (TAS-F), was effective in the desilylation of (−)-**50**, providing intermediate (−)-**52** in good yields (Scheme 5). We envisaged that the less bulky *o*-xylylene-based phosphate protecting group (XEPA) on phosphoramidite **54** [52,53] would be preferable for the phosphorylation of (−)-**52**. This protecting group is base stable and can be removed

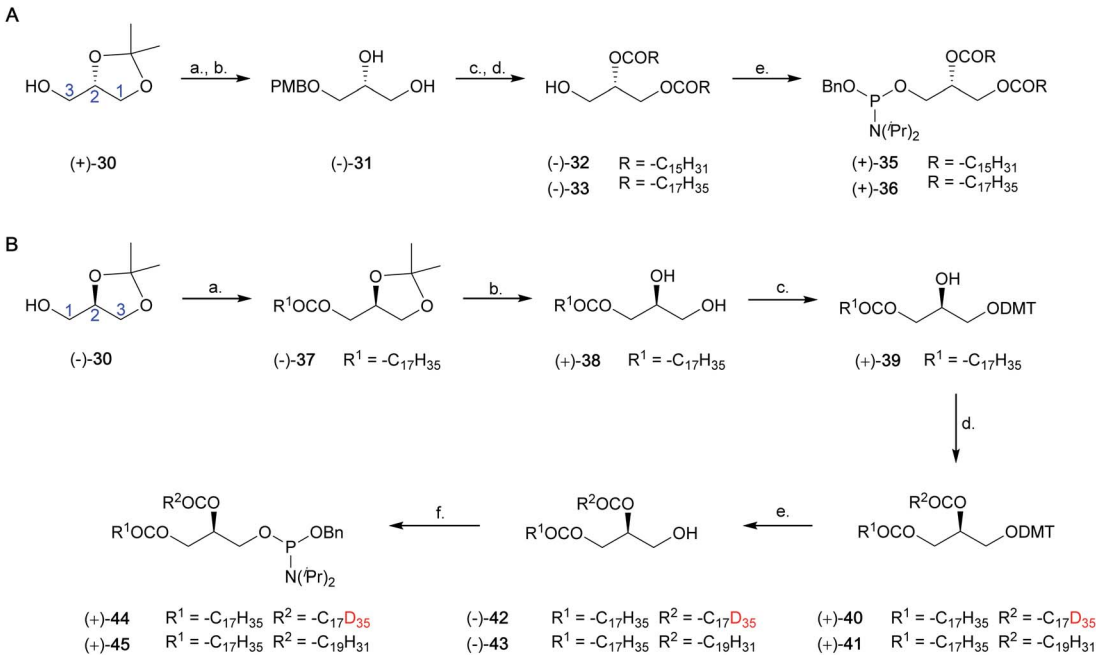

Scheme 4 Synthesis of a library of phosphoramidite fragments. (A) Synthesis of enantiomerically pure dipalmitoyl and distearoyl phosphoramidites (+)-**34** and (+)-**35**. *Reagents and conditions*: (a) (i) NaH, DMF, 0 °C to RT, 1 h, (ii) PMBCl, 0 °C to RT, 14 h, 98%. (b) PTSA·H_2O, MeOH, RT, 2 h, 81%. (c) Palmitoyl chloride or stearoyl chloride, pyridine, 4-DMAP, CH_2Cl_2, 0 °C to RT, 14 h, 91–99%. (d) 10% Pd/C, $H_{2(g)}$, EtOAc, RT, 2 h, 91–96%. (e) P(OBn)(N(^{i}Pr)$_2$)$_2$ **34**, 1*H*-tetrazole, CH_2Cl_2, RT, 19 h, 87–90%. (B) Synthesis of 1-*O*-stearoyl-2-*O*-(D_{35}-stearoyl)-*sn*-glycerol (−)-**44** and 1-*O*-stearoyl-2-*O*-(arachidonoyl)-*sn*-glycerol (−)-**45**. *Reagents and conditions*: (a) stearic acid, DCC, 4-DMAP, CH_2Cl_2, 0 °C to RT, 13 h, 76%. (b) AcOH/H_2O (4 : 1), 50 °C, 2 h, 70%, >99% e.e. (c) DMTCl, pyridine, RT, 50 min, 67%. (d) D_{35} stearic acid (Sigma Aldrich, 98 atom% D) or arachidonic acid, DCC, 4-DMAP, CH_2Cl_2, RT, 24 h, 91%, 70% D_{35}, 30% D_{34} (+)-**40**; 86% (+)-**41**. (e) AcOH/formic acid/H_2O (7 : 2 : 1), RT, 4 h, 94%, 72% D_{35}, 28% D_{34}, 95% e.e. (−)-**42**; 92%, 95% e.e. (+)-**43**. (f) P(OBn)(N(^{i}Pr)$_2$)$_2$ **34**, 1*H*-tetrazole, CH_2Cl_2, RT, 19 h, 90%, 70% D_{35}, 30% D_{34}, (+)-**44**; 88%, (+)-**45**. Ac = acetyl; Bn = benzyl; DCC = *N*,*N*′-dicyclohexylcarbodiimide; 4-DMAP = 4-dimethylaminopyridine; DMF = dimethylformamide; DMT = 4,4′-dimethoxytrityl; PMB = 4-methoxybenzyl; ✱ = deuterium.

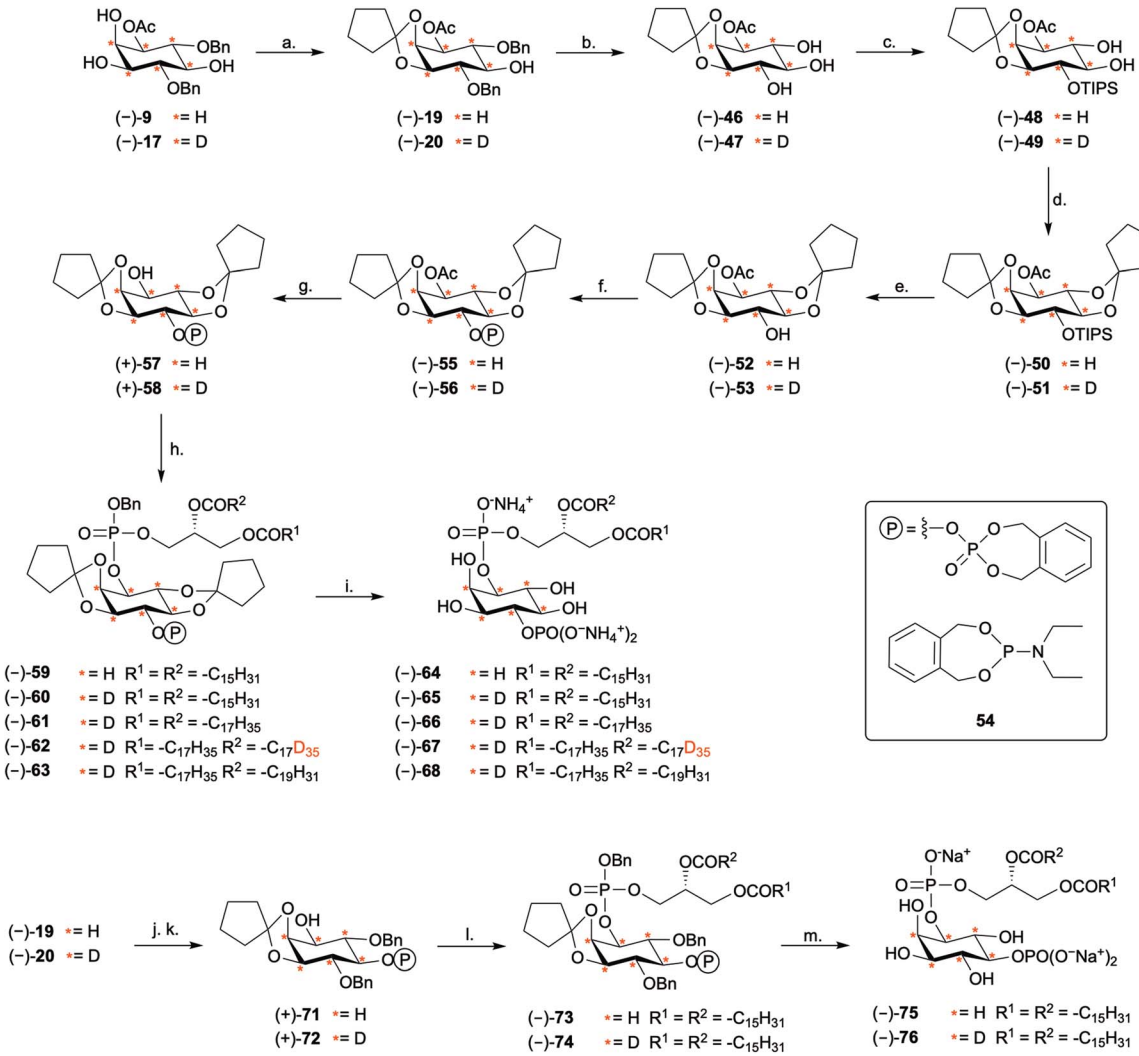

Scheme 5 Synthesis of PtdIns4*P* and PtdIns5*P* derivatives. *Reagents and conditions*: (a) 1,1-dimethoxycyclopentane **18**, PTSA·H_2O, CH_2Cl_2, RT, 18–19 h, 92% (−)-**19**; 87%, 91% D_6, 9% D_5 (−)-**20**. (b) 10% Pd/C, $H_{2(g)}$, EtOAc, RT, 2 h, 94% (−)-**46**; 76%, 84% D_6, 16% D_5 (−)-**47**. (c) TIPSOTf, 2,6-lutidine, THF, −78 °C, 16–16.5 h, 71% (−)-**48**; 74%, 84% D_6, 16% D_5 (−)-**49**. (d) 1,1-Dimethoxycyclopentane **18**, PTSA·H_2O, CH_2Cl_2, 30 °C, 16–18 h, 85% (−)-**50**; 71%, 85% D_6, 15% D_5 (−)-**51**. (e) TAS-F, DMF, RT, 1.5–3 h, 77% (−)-**52**; 88%, 84% D_6, 16% D_5 (−)-**53**. (f) (i) **54**, 1*H*-tetrazole, CH_2Cl_2, RT, 1–1.5 h, (ii) *m*CPBA, −78 °C to RT, 1.5 h, 79% (−)-**55**; 88%, 84% D_6, 16% D_5 (−)-**56**. (g) K_2CO_3, MeOH, RT, 1 h, 74% (+)-**57**; 86%, 84% D_6, 16% D_5 (+)-**58**. (h) (i) (+)-**35**, (+)-**36**, (+)-**44** or (+)-**45**, 1*H*-tetrazole, CH_2Cl_2, RT, 4–22 h, (ii) *m*CPBA, −78 °C to RT, 3–19 h, 55% (−)-**59**; 55% 87% D_6, 13% D_5 (−)-**60**; 64% 87% D_6, 13% D_5 (−)-**61**; 65%, 62% D_{41}, 29% D_{40}, 9% D_{39} (−)-**62**; 79%, 82% D_6, 18% D_5 (−)-**63**. (i) (i). TMSBr, toluene, RT, 12 h, (ii) MeOH, 0 °C, 1 h, 68% (−)-**64**; 75%, 86% D_6, 14% D_5 (−)-**65**; 36%, 84% D_6, 16% D_5 (−)-**66**; 58%, 59% D_{41}, 31% D_{40}, 10% D_{39} (−)-**67**; 53%, 86% D_6, 14% D_5 (−)-**68**. (j) (i) **54**, 1*H*-tetrazole, CH_2Cl_2, RT, 1 h, (ii) *m*CPBA, −78 °C to RT, 1.5 h, 92% (−)-**69**; 61%, 88% D_6, 12% D_5 (−)-**70** (k). K_2CO_3, MeOH, RT, 1 h, 74% (+)-**71**; 89%, 89% D_6, 11% D_5 (+)-**72**. (l) (i) (+)-**35** 1*H*-tetrazole, CH_2Cl_2, RT, 20–22 h, (ii) *m*CPBA, −78 °C to RT, 3–4 h, 82% (−)-**73**; 46%, 88% D_6, 12% D_5 (−)-**74**. (m) (i) Pd black, $H_{2(g)}$, ^{t}BuOH/H_2O, RT, 17–21 h, (ii) $NaHCO_3$, RT, 4 h or 2 min, 94% (−)-**75**; 86%, 90% D_6, 10% D_5 (−)-**76**. Ac = acetyl; Bn = benzyl; DMF = dimethylformamide; *m*CPBA = *meta*-chloroperoxybenzoic acid; PTSA = 4-toluene sulfonic acid; TAS-F = tris(dimethylamino)sulfonium difluorotrimethylsilicate; Tf = triflyl; TIPS = triisopropylsilyl; TMS = tetramethylsilane; ✱ = deuterium.

simultaneously to acid-labile groups *via* hydrogenolysis or using TMSBr.[33] Therefore, phosphitylation of (−)-**52** was carried out with three equivalents of **54** in the presence of 1*H*-tetrazole, followed by *m*CPBA oxidation of the intermediate, providing (−)-**55** in excellent yield. Subsequent deacetylation under standard basic conditions furnished alcohol (−)-**57** (Scheme 5).

Coupling of the inositol core (−)-**57** to the phosphoramidite fragment (+)-**35** provided the corresponding phosphite intermediate and oxidation with *m*CPBA yielded the fully-protected inositol intermediate (−)-**59**. Final global deprotection was then achieved by treatment with TMSBr in toluene. Methanolysis of the resulting silyl phosphate esters was accomplished by stirring the residue obtained in MeOH at 0 °C for 1 hour. Purification using column chromatography over silica gel[33,54] furnished PtdIns4*P* (−)-**64** as its presumed ammonium salt, in 68% yield (Scheme 5).

To validate the versatility of the route developed, we synthesised the equivalent D_6-core, (−)-**58,** starting from D_6-*myo*-inositol (Scheme 5). We used ^{2}H NMR and 2D NMR to characterise the deuterated compounds, as compared to their

protonated counterparts (Fig. S5†). Subsequent coupling of (−)-**58** to phosphoramidites (+)-**35**, (+)-**36**, (+)-**44** and (+)-**45**, provided a range of H_6- and D_6-PtdIns4*P* derivatives (Scheme 5), including D_6-dipalmitoyl PtdIns4*P* (−)-**65** (86% D_6, 14% D_5), D_6-distearoyl PtdIns4*P* (−)-**66** (84% D_6, 16% D_5), D_{41}-distearoyl PtdIns4*P* (−)-**67** (59% D_{41}, 31% D_{40}, 10% D_{39}), and D_6-1-stearoyl-2-arachidonoyl PtdIns4*P* (−)-**68** (86% D_6, 14% D_5).

The versatility of our synthetic approach was further demonstrated by the synthesis of H_6- and D_6-PtdIns5*P* derivatives. The synthesis started from the key inositol building blocks (−)-**19** and (−)-**20** and proceeded *via* a sequence of steps similar to those outlined in the synthesis of PtdIns4*P* analogues. Phosphitylation with excess XEPA **54** and catalytic 1*H*-tetrazole followed by *m*CPBA oxidation and deacetylation, furnished (+)-**71** and (+)-**72** in excellent yields. Assembly of these inositol precursors with phosphoramidite (+)-**35** gave the fully protected PtdInsP_ns (−)-**73** and (−)-**74**. Global deprotection of these precursors was accomplished using palladium black-catalysed hydrogenolysis in a mixture of ^{t}BuOH and H_2O. Conveniently, these conditions were found to cleave all protecting groups, including the acid-labile 2,3-*O*-cyclopentylidene acetal to give dipalmitoyl PtdIns5*P* (−)-**75** and (−)-**76**, as their presumed sodium salt. Importantly, the D_6-PtdIns4*P* and PtdIns5*P* derivatives synthesised revealed a distinct shift of +6 mass units when analysed by high resolution mass-spectrometry (Fig. S6 and S7†), as compared to their protonated counterpart, as well as a loss of the ^{1}H NMR signals corresponding to *myo*-inositol headgroup protons (Fig. S8 and S9†).

The synthetic route optimised in this work therefore enables the synthesis of a range of isotopically-labelled, saturated and unsaturated, PtdIns4*P* and PtdIns5*P* derivatives in 13 and 8 steps, respectively, using an enzymatic desymmetrisation strategy.

Deuterated PtdInsP_ns (−)-65, (−)-67, and (−)-76 to probe intracellular levels of the endogenous phospholipids

Finally, we investigated whether the deuterated PtdInsP_ns (−)-65, (−)-**67**, and (−)-**76** could be used to probe intracellular levels of the endogenous phospholipids. Each deuterated probe was delivered into MCF-7 cells by forming a complex with the polyamine carrier neomycin B sulfate, as previously described.[55] The complexes of deuterated PtdInsP_n and carrier were incubated with MCF-7 cells for 1 h. Following extraction, the deuterated and endogenous PtdInsP_n species were quantified using LC-MS.[22] Each deuterated PtdInsP_n probe was clearly detected following extraction from the MCF-7 cells that had been treated with the complex. In contrast, the deuterated probes were not detected in the carrier only and untreated controls (Fig. 3A). The level of detected deuterated PtdInsP_n probe was found to be directly proportional to the concentration of the PtdInsP_n/carrier complex with which the MCF-7 cells were treated. In addition, the level of each deuterated PtdInsP_n probe detected from the MCF-7 cells was higher than the level of endogenous PtdInsP_n species detected in the MCF-7 cells under these conditions (Fig. 3B). Importantly, the mass shift of +6 afforded by the D_6-labelled PtdInsP_n is sufficient to avoid interference with the signal for the endogenous species, even when the probe is in large excess and has the same LC retention time. Overall, these data demonstrate that the deuterated PtdIns4*P* derivative (−)-65, and the deuterated PtdIns5*P*

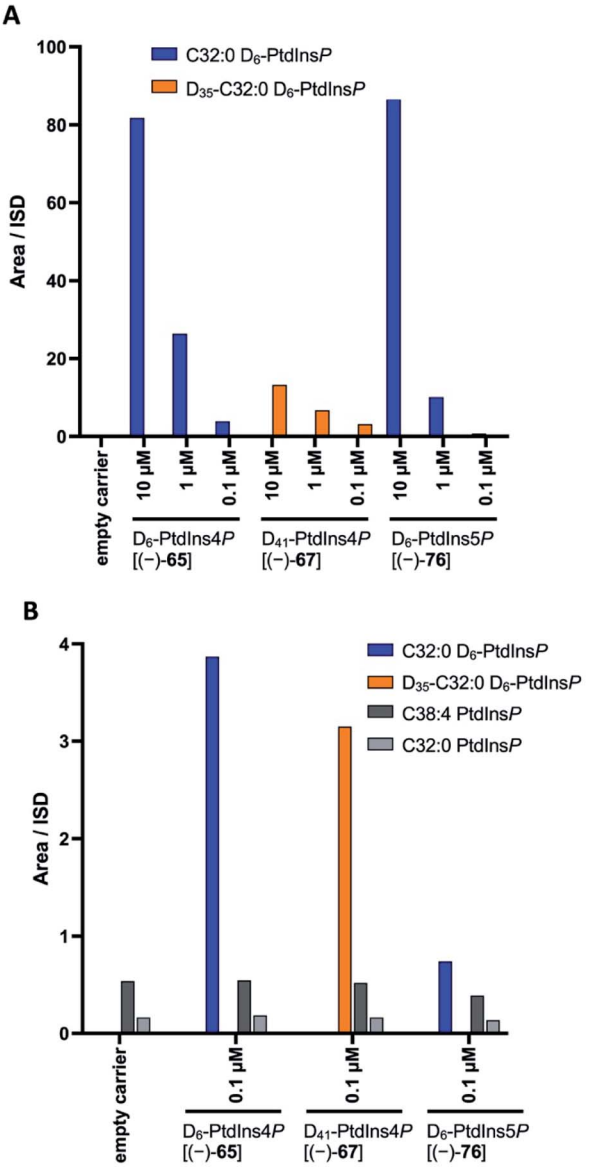

Fig. 3 Delivery of D_6-PtdInd4*P* [(−)-**65**], D_{41}-PtdInd4*P* [(−)-**67**,] and D_6-PtdIns5*P* [(−)-**76**] to MCF-7 cells by a polyamine carrier and detection of deuterated and endogenous PtdIndP_ns using LC-MS. (A) Serum starved MCF-7 cells were treated with a complex of each deuterated PtdInsP_n and the polyamine carrier neomycin B sulfate for 1 h. The final concentration for both PtdInsP_n and carrier was 10 μM, 1 μM or 0.1 μM. Control cells were either untreated or treated with the polyamine carrier for 1 h at a final concentration of 1 μM. The levels of D_6-PtdInd4*P* [(−)-**65**], D_{41}-PtdInd4*P* [(−)-**67**], and D_6-PtdIns5*P* [(−)-**76**] in the indicated treatment conditions are presented as their peak area relative to the internal standard. (B) Serum starved MCF-7 cells were treated with a complex of each deuterated PtdInsP_n and the polyamine carrier neomycin B sulfate for 1 h. The final concentration for both PtdInsP_n and carrier was 0.1 μM. Control cells were either untreated or treated with the polyamine carrier for 1 h at a final concentration of 0.1 μM. The levels of D_6-PtdInd4*P* [(−)-**65**], D_{41}-PtdInd4*P* [(−)-**67**], D_6-PtdIns5*P* [(−)-**76**], and endogenous C38:4 and C32:0 in the indicated treatment conditions are presented as their peak area relative to the internal standard.

derivative (−)-76, are powerful probes for quantifying intracellular levels of endogenous PtdInsP_ns. These compounds will be important in furthering our understanding of the biological role of these important signalling molecules.

Conclusions

In summary, we have developed robust, and efficient synthetic routes towards saturated and unsaturated PtdIns4*P* and PtdIns5*P* derivatives. To our knowledge, this work represents both the first synthesis of unsaturated PtdIns4*P* derivatives that relies on a desymmetrisation strategy,[28–30] and the most efficient synthesis of enantiomerically pure PtdIns5*P* described so far, with an overall yield of 20%.[35,56,57] As a result of the high yielding enzymatic desymmetrisation strategy employed, these routes are amenable to the synthesis of a versatile set of stable-isotope labelled PtdIns*P* derivatives. This is demonstrated through the optimisation of a large-scale synthesis of deuterated *myo*-inositol, and the synthesis of a set of deuterated PtdIns4*P* and PtdIns5*P* derivatives. In addition to the deuterated analogues synthesised herein, this synthetic route could be readily extended to the synthesis of [^{13}C]-labelled PtdIns*P* derivatives.[25]

We have demonstrated that the stable isotope-labelled PtdInsP_n probes synthesised represent powerful tools for quantifying PtdInsP_n levels in a cellular setting. Application of these compounds to MCF7 cells enable quantification of endogenous PtdInsP_n levels in a manner that was previously impossible. Further applications for these probes include their use as exogenously-supplied tracers for PtdInsP_n metabolism. In addition, isotopically-labelled PtdInsP_ns could reveal positional isomer-specific details of the phospholipid metabolism, using previously developed HPLC-MS-based methods.[22] Finally, the C–D bond has been recognised as an ideal bioorthogonal chemical label for highly sensitive imaging techniques, including stimulated Raman scattering (SRS)[58,59] and hyperspectral SRS (hsSRS) microscopy. These innovative technologies could allow quantitative imaging of isotopically-labelled PtdInsP_n *in vitro* and *in vivo* with subcellular resolution.[26,27,60] Therefore, important information regarding the dynamics and intracellular spatial localisation of PtdInsP_n in living cells and organisms could be obtained using these isotopically-labelled probes.

Overall, the efficient synthetic routes developed gave deuterated PtdInsP_n, which were validated as powerful probes for determining cellular levels of endogenous PtdInsP_n. This work promises to significantly expand the scope of isotopically-labelled PtdInsP_n probes available to the scientific community, which will enable a deeper understanding of PtdInsP_n metabolism and biology.

Conflicts of interest

There are no conflicts to declare.

Acknowledgements

A. M. J. thanks the EPSRC and AstraZeneca for the award of an iCASE studentship, and the EPSRC for the award of an EPSRC Doctoral Prize (EP/N509711/1). A. M. S was supported by the EPSRC and the MRC through the Systems Approaches to Biomedical Sciences Doctoral Training Centre (EP/G037280/1) with additional support from AstraZeneca. We thank Dr James Wickens from the CRL Mass Spectrometry Research Facility, Dr Barbara O'Dell and Tina Jackson from the CRL NMR Research Facility at the University of Oxford. S. J. C. thanks St Hugh's College, Oxford, for research support.

Notes and references

1 E. J. Dickson and B. Hille, *Biochem. J.*, 2019, **476**, 1–23.
2 T. Balla, *Physiol. Rev.*, 2013, **93**, 1019–1137.
3 D. M. Brown, B. F. C. Clark, G. E. Hall and R. Letters, *Proc. Chem. Soc*, 1960, 212–213.
4 T. Sasaki, S. Takasuga, J. Sasaki, S. Kofuji, S. Eguchi, M. Yamazaki and A. Suzuki, *Prog. Lipid Res.*, 2009, **48**, 307–343.
5 T. Balla, *Curr. Pharm. Des.*, 2001, **7**, 475–507.
6 G. Di Paolo and P. De Camilli, *Nature*, 2006, **443**, 651–657.
7 M. A. Lemmon, *Nat. Rev. Mol. Cell Biol.*, 2008, **9**, 99–111.
8 M. R. Wenk and P. De Camilli, *Proc. Natl. Acad. Sci. U. S. A.*, 2004, **101**, 8262–8269.
9 J. Viaud, R. Mansour, A. Antkowiak, A. Mujalli, C. Valet, G. Chicanne, J.-M. Xuereb, A.-D. Terrisse, S. Severin, M.-P. Gratacap, F. Gaits-Iacovoni and B. Payrastre, *Biochimie*, 2016, **125**, 250–258.
10 R. Behnia and S. Munro, *Nature*, 2005, **438**, 597–604.
11 J. E. Burke, *Mol. Cell*, 2018, **71**, 653–673.
12 E. Boura and R. Nencka, *Exp. Cell Res.*, 2015, **337**, 136–145.
13 N. Altan-Bonnet, *Trends Cell Biol.*, 2017, **27**, 201–213.
14 J. Tan and J. A. Brill, *Crit. Rev. Biochem. Mol. Biol.*, 2014, **49**, 33–58.
15 A. Poli, A. E. Zaurito, S. Abdul-Hamid, R. Fiume, I. Faenza and N. Divecha, *Int. J. Mol. Sci.*, 2019, **20**, 2080.
16 M. D. Best, H. Zhang and G. D. Prestwich, *Nat. Prod. Rep.*, 2010, **27**, 1403–1430.
17 M. D. Best, *Chem. Phys. Lipids*, 2014, **182**, 19–28.
18 S. J. Conway and G. J. Miller, *Nat. Prod. Rep.*, 2007, **24**, 687–707.
19 G. D. Prestwich, *Chem. Biol.*, 2004, **11**, 619–637.
20 J. C. Bozelli and R. M. Epand, *Proteomics*, 2019, **19**, 1900138.
21 T. Kimura, W. Jennings and R. M. Epand, *Prog. Lipid Res.*, 2016, **62**, 75–92.
22 J. Clark, K. E. Anderson, V. Juvin, T. S. Smith, F. Karpe, M. J. O. Wakelam, L. R. Stephens and P. T. Hawkins, *Nat. Methods*, 2011, **8**, 267–272.
23 A. Kielkowska, I. Niewczas, K. E. Anderson, T. N. Durrant, J. Clark, L. R. Stephens and P. T. Hawkins, *Adv. Biol. Regul.*, 2014, **54**, 131–141.
24 C. H. Johnson, J. Ivanisevic and G. Siuzdak, *Nat. Rev. Mol. Cell Biol.*, 2016, **17**, 451–459.
25 R. K. Harmel, R. Puschmann, M. N. Trung, A. Saiardi, P. Schmieder and D. Fiedler, *Chem. Sci.*, 2019, **10**, 5267–5274.
26 L. Zhang, L. Shi, Y. Shen, Y. Miao, M. Wei, N. Qian, Y. Liu and W. Min, *Nat. Biomed. Eng.*, 2019, **3**, 402–413.
27 F. Hu, L. Shi and W. Min, *Nat. Methods*, 2019, **16**, 830–842.

28 S. Furse, L. Mak, E. W. Tate, R. H. Templer, O. Ces, R. Woscholski and P. R. J. Gaffney, *Org. Biomol. Chem.*, 2015, **13**, 2001–2011.
29 J. He, J. Gajewiak, J. L. Scott, D. Gong, M. Ali, M. D. Best, G. D. Prestwich, R. V. Stahelin and T. G. Kutateladze, *Chem. Biol.*, 2011, **18**, 1312–1319.
30 W. Huang, H. Zhang, F. Davrazou, T. G. Kutateladze, X. Shi, O. Gozani and G. D. Prestwich, *J. Am. Chem. Soc.*, 2007, **129**, 6498–6506.
31 Y. Watanabe and H. Ishikawa, *Tetrahedron Lett.*, 2000, **41**, 8509–8512.
32 S. J. Conway, J. Gardiner, S. J. A. Grove, M. K. Johns, Z.-Y. Lim, G. F. Painter, D. E. J. E. Robinson, C. Schieber, J. W. Thuring, L. S. M. Wong, M.-X. Yin, A. W. Burgess, B. Catimel, P. T. Hawkins, N. T. Ktistakis, L. R. Stephens and A. B. Holmes, *Org. Biomol. Chem.*, 2010, **8**, 66–76.
33 B. R. Sculimbrene, Y. Xu and S. J. Miller, *J. Am. Chem. Soc.*, 2004, **126**, 13182–13183.
34 B. R. Sculimbrene, A. J. Morgan and S. J. Miller, *Chem. Commun.*, 2003, 1781–1785.
35 K. J. Kayser-Bricker, P. A. Jordan and S. J. Miller, *Tetrahedron*, 2008, **64**, 7015–7020.
36 M. F. P. Ribeiro, K. C. Pais, B. S. M. de Jesus, R. Fernandez-Lafuente, D. M. G. Freire, E. A. Manoel and A. B. C. Simas, *Eur. J. Org. Chem.*, 2018, **2018**, 386–391.
37 M. G. Vasconcelos, R. H. C. Briggs, L. C. S. Aguiar, D. M. G. Freire and A. B. C. Simas, *Carbohydr. Res.*, 2014, **386**, 7–11.
38 M. B. Lauber, C.-G. Daniliuc and J. Paradies, *Chem. Commun.*, 2013, **49**, 7409–7411.
39 B. R. Sculimbrene and S. J. Miller, *J. Am. Chem. Soc.*, 2001, **123**, 10125–10126.
40 X. Wang, M. Barrett, J. Sondek, T. K. Harden and Q. Zhang, *Biochemistry*, 2012, **51**, 5300–5306.
41 P. J. Kocienski, *Protecting Groups, 3rd edition 2005*, Georg Thieme Verlag, Stuttgart, 3rd edn, 2014.
42 I. H. Gilbert, A. B. Holmes and R. C. Young, *Tetrahedron Lett.*, 1990, **31**, 2633–2634.
43 D. C. Billington and R. Baker, *Chem. Commun.*, 1987, 1011.
44 D. C. Billington, R. Baker, J. J. Kulagowski, I. M. Mawer, J. P. Vacca, S. J. deSolms and J. R. Huff, *J. Chem. Soc., Perkin Trans. 1*, 1989, 1423–1429.
45 R. Fernandez-Lafuente, *J. Mol. Catal. B: Enzym.*, 2010, **62**, 197–212.
46 J. M. Seco, E. Quiñoá and R. Riguera, *Chem. Rev.*, 2004, **104**, 17–118.
47 K. Laumen and O. Ghisalba, *Biosci., Biotechnol., Biochem.*, 1994, **58**, 2046–2049.
48 K. Sasaki, F. Balza and I. Taylor, *Carbohydr. Res.*, 1987, **166**, 171–180.
49 H. Zimmermann, *Liq. Cryst.*, 1989, **4**, 591–618.
50 T. Saito, K. Ikemoto, H. Tsunomachi and K. Sakaguchi, *US Pat.*, 4973720, 1990.
51 B. M. Trost, D. E. Patterson and E. J. Hembre, *J. Am. Chem. Soc.*, 1999, **121**, 10834–10835.
52 Y. Watanabe, Y. Komoda, K. Ebisuya and S. Ozaki, *Tetrahedron Lett.*, 1990, **31**, 255–256.
53 M. Gregory, B. Catimel, M.-X. Yin, M. Condron, A. Burgess and A. B. Holmes, *Synlett*, 2015, **27**, 121–125.
54 K. R. Auger, C. L. Carpenter, L. C. Cantley and L. Varticovski, *J. Biol. Chem.*, 1989, **264**, 20181–20184.
55 S. Ozaki, D. B. DeWald, J. C. Shope, J. Chen and G. D. Prestwich, *Proc. Natl. Acad. Sci. U. S. A.*, 2000, **97**, 11286–11291.
56 J. Peng and G. D. Prestwich, *Tetrahedron Lett.*, 1998, **39**, 3965–3968.
57 J. R. Falck, U. M. Krishna, K. R. Katipally, J. H. Capdevila and E. T. Ulug, *Tetrahedron Lett.*, 2000, **41**, 4271–4275.
58 C. W. Freudiger, W. Min, B. G. Saar, S. Lu, G. R. Holtom, C. He, J. C. Tsai, J. X. Kang and X. S. Xie, *Science*, 2008, **322**, 1857–1861.
59 J. X. Cheng and X. S. Xie, *Science*, 2015, **350**, aaa8870.
60 D. Fu, Y. Yu, A. Folick, E. Currie, R. V. Farese, T.-H. Tsai, X. S. Xie and M. C. Wang, *J. Am. Chem. Soc.*, 2014, **136**, 8820–8828.